

Dual Attention Network for Scene Segmentation

Jun Fu^{1,3} Jing Liu*¹ Haijie Tian¹ Yong Li²
Yongjun Bao² Zhiwei Fang^{1,3} Hanqing Lu¹

¹National Laboratory of Pattern Recognition, Institute of Automation, Chinese Academy of Sciences

²Business Growth BU, JD.com ³ University of Chinese Academy of Sciences

{jun.fu, jliu, zhiwei.fang, luhq}@nlpr.ia.ac.cn, hjtian.bit@163.com, {liyong5, baoyongjun}@jd.com

Abstract

In this paper, we address the scene segmentation task by capturing rich contextual dependencies based on the self-attention mechanism. Unlike previous works that capture contexts by multi-scale feature fusion, we propose a Dual Attention Network (DANet) to adaptively integrate local features with their global dependencies. Specifically, we append two types of attention modules on top of dilated FCN, which model the semantic interdependencies in spatial and channel dimensions respectively. The position attention module selectively aggregates the feature at each position by a weighted sum of the features at all positions. Similar features would be related to each other regardless of their distances. Meanwhile, the channel attention module selectively emphasizes interdependent channel maps by integrating associated features among all channel maps. We sum the outputs of the two attention modules to further improve feature representation which contributes to more precise segmentation results. We achieve new state-of-the-art segmentation performance on three challenging scene segmentation datasets, i.e., Cityscapes, PASCAL Context and COCO Stuff dataset. In particular, a Mean IoU score of 81.5% on Cityscapes test set is achieved without using coarse data.¹

1. Introduction

Scene segmentation is a fundamental and challenging problem, whose goal is to segment and parse a scene image into different image regions associated with semantic categories including stuff (e.g. sky, road, grass) and discrete objects (e.g. person, car, bicycle). The study of this



Figure 1: The goal of scene segmentation is to recognize each pixel including stuff, diverse objects. The various scales, occlusion and illumination changing of objects/stuff make it challenging to parsing each pixel.

task can be applied to potential applications, such as automatic driving, robot sensing and image editing. In order to accomplish the task of scene segmentation effectively, we need to distinguish some confusing categories and take into account objects with different appearance. For example, regions of 'field' and 'grass' are often indistinguishable, and the objects of 'cars' may often be affected by scales, occlusion and illumination. Therefore, it is necessary to enhance the discriminative ability of feature representations for pixel-level recognition.

Recently, state-of-the-art methods based on Fully Convolutional Networks (FCNs) [13] have been proposed to address the above issues. One way is to utilize the multi-scale context fusion. For example, some works [3, 4, 30] aggregate multi-scale contexts via combining feature maps generated by different dilated convolutions and pooling operations. And some works [15, 28] capture richer global context information by enlarging the kernel size with a decomposed structure or introducing an effective encoding layer on top of the network. In addition, the encoder-decoder

*Corresponding Author

¹Links can be found at <https://github.com/junfu1115/DANet/>

structures [6, 10, 16] are proposed to fuse mid-level and high-level semantic features. Although the context fusion helps to capture different scales objects, it can not leverage the relationship between objects or stuff in a global view, which is also essential to scene segmentation.

Another type of methods employs recurrent neural networks to exploit long-range dependencies, thus improving scene segmentation accuracy. The method based on 2D LSTM networks [1] is proposed to capture complex spatial dependencies on labels. The work [18] builds a recurrent neural network with directed acyclic graph to capture the rich contextual dependencies over local features. However, these methods capture the global relationship implicitly with recurrent neural networks, whose effectiveness relies heavily on the learning outcome of the long-term memorization.

To address above problems, we propose a novel framework, called as Dual Attention Network (DANet), for natural scene image segmentation, which is illustrated in Figure. 2. It introduces a self-attention mechanism to capture features dependencies in the spatial and channel dimensions respectively. Specifically, we append two parallel attention modules on top of dilated FCN. One is a *position attention module* and the other is a *channel attention module*. For the position attention module, we introduce the self-attention mechanism to capture the spatial dependencies between any two positions of the feature maps. For the feature at a certain position, it is updated via aggregating features at all positions with weighted summation, where the weights are decided by the feature similarities between the corresponding two positions. That is, any two positions with similar features can contribute mutual improvement regardless of their distance in spatial dimension. For the channel attention module, we use the similar self-attention mechanism to capture the channel dependencies between any two channel maps, and update each channel map with a weighted sum of all channel maps. Finally, the outputs of these two attention modules are fused to further enhance the feature representations.

It should be noted that our method is more effective and flexible than previous methods [4, 30] when dealing with complex and diverse scenes. Take the street scene in Figure. 1 as an example. First, some 'person' and 'traffic light' in the first row are inconspicuous or incomplete objects due to lighting and view. If simple contextual embedding is explored, the context from dominated salient objects (e.g. car, building) would harm those inconspicuous object labeling. By contrast, our attention model selectively aggregates the similar features of inconspicuous objects to highlight their feature representations and avoid the influence of salient objects. Second, the scales of the 'car' and 'person' are diverse, and recognizing such diverse objects requires contextual information at different scales. That is, the features

at different scale should be treated equally to represent the same semantics. Our model with attention mechanism just aims to adaptively integrate similar features at any scales from a global view, and this can solve the above problem to some extent. Third, we explicitly take spatial and channel relationships into consideration, so that scene understanding could benefit from long-range dependencies.

Our main contributions can be summarized as follows:

- We propose a novel Dual Attention Network (DANet) with self-attention mechanism to enhance the discriminant ability of feature representations for scene segmentation.
- A position attention module is proposed to learn the spatial interdependencies of features and a channel attention module is designed to model channel interdependencies. It significantly improves the segmentation results by modeling rich contextual dependencies over local features.
- We achieve new state-of-the-art results on three popular benchmarks including Cityscapes dataset [5], PASCAL Context dataset [14] and COCO Stuff dataset [2].

2. Related Work

Semantic Segmentation. Fully Convolutional Networks (FCNs) based methods have made great progress in semantic segmentation. There are several model variants proposed to enhance contextual aggregation. First, Deeplabv2 [3] and Deeplabv3 [4] adopt atrous spatial pyramid pooling to embed contextual information, which consist of parallel dilated convolutions with different dilated rates. PSPNet [30] designs a pyramid pooling module to collect the effective contextual prior, containing information of different scales. The encoder-decoder structures [?, 6, 8, 9] fuse mid-level and high-level semantic features to obtain different scale context. Second, learning contextual dependencies over local features also contribute to feature representations. DAG-RNN [18] models directed acyclic graph with recurrent neural network to capture the rich contextual dependencies. PSANet [31] captures pixel-wise relation by a convolution layer and relative position information in spatial dimension. The concurrent work OCNet [27] adopts self-attention mechanism with ASPP to exploit context dependencies. In addition, EncNet [28] introduces a channel attention mechanism to capture global context.

Self-attention Modules. Attention modules can model long-range dependencies and have been widely applied in many tasks [11, 12, 17, 19–21]. In particular, the work [21] is the first to propose the self-attention mechanism to draw global dependencies of inputs and applies it in machine translation. Meanwhile, attention modules are increasingly

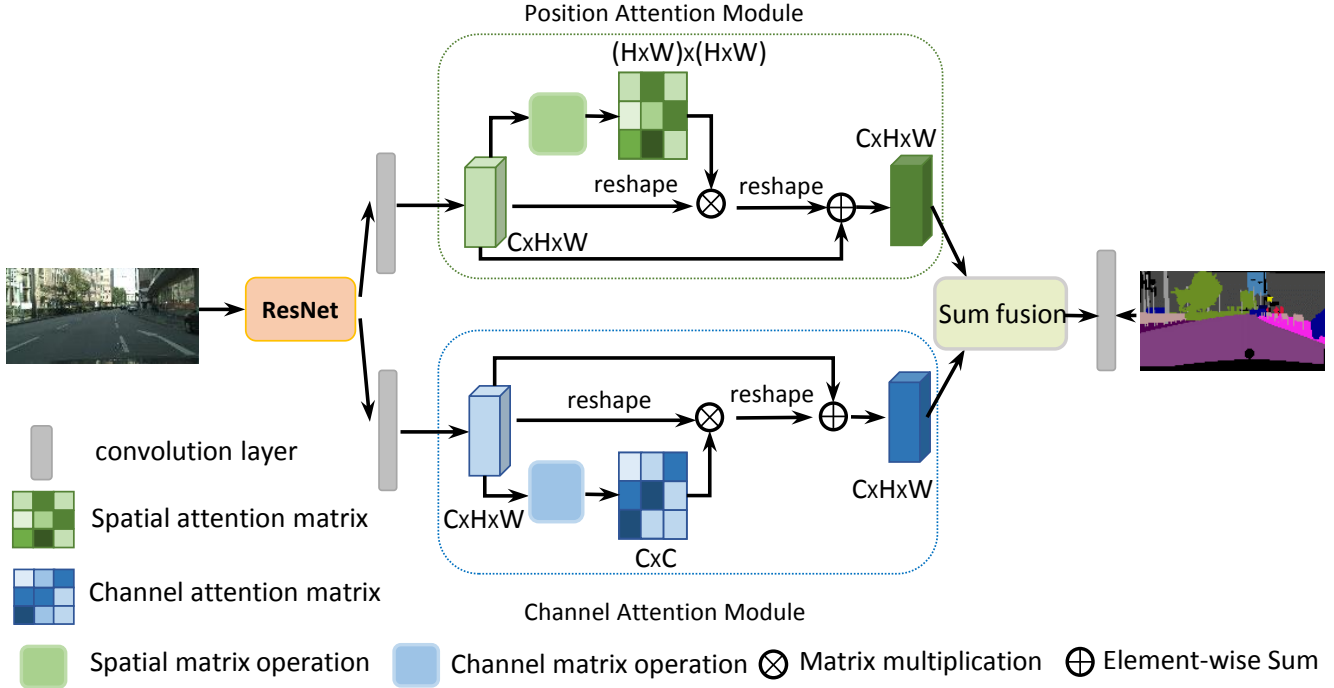


Figure 2: An overview of the Dual Attention Network. (Best viewed in color)

applied in image vision field. The work [29] introduces self-attention mechanism to learn a better image generator. The work [23], which is related to self-attention module, mainly exploring effectiveness of non-local operation in spacetime dimension for videos and images.

Different from previous works, we extend the self-attention mechanism in the task of scene segmentation, and carefully design two types of attention modules to capture rich contextual relationships for better feature representations with intra-class compactness. Comprehensive empirical results verify the effectiveness of our proposed method.

3. Dual Attention Network

In this section, we first present a general framework of our network and then introduce the two attention modules which capture long-range contextual information in spatial and channel dimension respectively. Finally we describe how to aggregate them together for further refinement.

3.1. Overview

Given a picture of scene segmentation, stuff or objects, are diverse on scales, lighting, and views. Since convolution operations would lead to a local receptive field, the features corresponding to the pixels with the same label may have some differences. These differences introduce intra-class inconsistency and affect the recognition accuracy. To address this issue, we explore global contextual information by building associations among features with the attention

mechanism. Our method could adaptively aggregate long-range contextual information, thus improving feature representation for scene segmentation.

As illustrated in Figure. 2, we design two types of attention modules to draw global context over local features generated by a dilated residual network, thus obtaining better feature representations for pixel-level prediction. We employ a pretrained residual network with the dilated strategy [3] as the backbone. Noted that we remove the downsampling operations and employ dilated convolutions in the last two ResNet blocks, thus enlarging the size of the final feature map size to $1/8$ of the input image. It retains more details without adding extra parameters. Then the features from the dilated residual network would be fed into two parallel attention modules. Take the spatial attention modules in the upper part of the Figure. 2 as an example, we first apply a convolution layer to obtain the features of dimension reduction. Then we feed the features into the position attention module and generate new features of spatial long-range contextual information through the following three steps. The first step is to generate a spatial attention matrix which models the spatial relationship between any two pixels of the features. Next, we perform a matrix multiplication between the attention matrix and the original features. Third, we perform an element-wise sum operation on the above multiplied resulting matrix and original features to obtain the final representations reflecting long-range contexts. Meanwhile, long-range contextual informa-

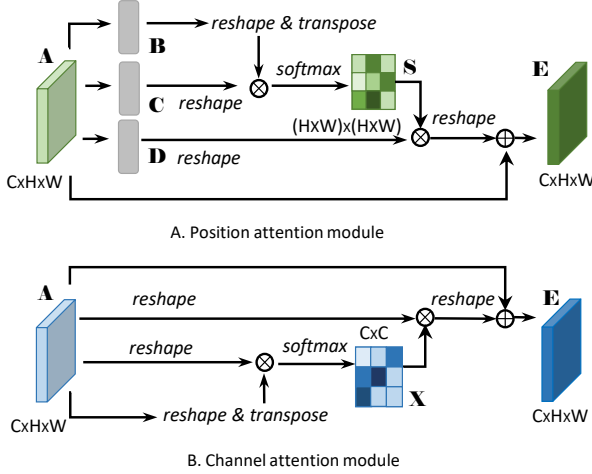


Figure 3: The details of Position Attention Module and Channel Attention Module are illustrated in (A) and (B). (Best viewed in color)

tion in channel dimension are captured by a channel attention module. The process of capturing the channel relationship is similar to the position attention module except for the first step, in which channel attention matrix is calculated in channel dimension. Finally we aggregate the outputs from the two attention modules to obtain better feature representations for pixel-level prediction.

3.2. Position Attention Module

Discriminant feature representations are essential for scene understanding, which could be obtained by capturing long-range contextual information. However, many works [15, 30] suggest that local features generated by traditional FCNs could lead to misclassification of objects and stuff. In order to model rich contextual relationships over local features, we introduce a position attention module. The position attention module encodes a wider range of contextual information into local features, thus enhancing their representation capability. Next, we elaborate the process to adaptively aggregate spatial contexts.

As illustrated in Figure.3(A), given a local feature $A \in \mathbb{R}^{C \times H \times W}$, we first feed it into a convolution layers to generate two new feature maps B and C , respectively, where $\{B, C\} \in \mathbb{R}^{C \times H \times W}$. Then we reshape them to $\mathbb{R}^{C \times N}$, where $N = H \times W$ is the number of pixels. After that we perform a matrix multiplication between the transpose of C and B , and apply a softmax layer to calculate the spatial attention map $S \in \mathbb{R}^{N \times N}$:

$$s_{ji} = \frac{\exp(B_i \cdot C_j)}{\sum_{i=1}^N \exp(B_i \cdot C_j)} \quad (1)$$

where s_{ji} measures the i^{th} position's impact on j^{th} position. The more similar feature representations of the two

position contributes to greater correlation between them.

Meanwhile, we feed feature A into a convolution layer to generate a new feature map $D \in \mathbb{R}^{C \times H \times W}$ and reshape it to $\mathbb{R}^{C \times N}$. Then we perform a matrix multiplication between D and the transpose of S and reshape the result to $\mathbb{R}^{C \times H \times W}$. Finally, we multiply it by a scale parameter α and perform an element-wise sum operation with the features A to obtain the final output $E \in \mathbb{R}^{C \times H \times W}$ as follows:

$$E_j = \alpha \sum_{i=1}^N (s_{ji} D_i) + A_j \quad (2)$$

where α is initialized as 0 and gradually learns to assign more weight [29]. It can be inferred from Equation 2 that the resulting feature E at each position is a weighted sum of the features across all positions and original features. Therefore, it has a global contextual view and selectively aggregates contexts according to the spatial attention map. The similar semantic features achieve mutual gains, thus improving intra-class compact and semantic consistency.

3.3. Channel Attention Module

Each channel map of high level features can be regarded as a class-specific response, and different semantic responses are associated with each other. By exploiting the interdependencies between channel maps, we could emphasize interdependent feature maps and improve the feature representation of specific semantics. Therefore, we build a channel attention module to explicitly model interdependencies between channels.

The structure of channel attention module is illustrated in Figure.3(B). Different from the position attention module, we directly calculate the channel attention map $X \in \mathbb{R}^{C \times C}$ from the original features $A \in \mathbb{R}^{C \times H \times W}$. Specifically, we reshape A to $\mathbb{R}^{C \times N}$, and then perform a matrix multiplication between A and the transpose of A . Finally, we apply a softmax layer to obtain the channel attention map $X \in \mathbb{R}^{C \times C}$:

$$x_{ji} = \frac{\exp(A_i \cdot A_j)}{\sum_{i=1}^C \exp(A_i \cdot A_j)} \quad (3)$$

where x_{ji} measures the i^{th} channel's impact on the j^{th} channel. In addition, we perform a matrix multiplication between the transpose of X and A and reshape their result to $\mathbb{R}^{C \times H \times W}$. Then we multiply the result by a scale parameter β and perform an element-wise sum operation with A to obtain the final output $E \in \mathbb{R}^{C \times H \times W}$:

$$E_j = \beta \sum_{i=1}^C (x_{ji} A_i) + A_j \quad (4)$$

where β gradually learns a weight from 0. The Equation 4 shows that the final feature of each channel is a weighted

sum of the features of all channels and original features, which models the long-range semantic dependencies between feature maps. It helps to boost feature discriminability.

Noted that we do not employ convolution layers to embed features before computing relationships of two channels, since it can maintain relationship between different channel maps. In addition, different from recent works [28] which explores channel relationships by a global pooling or encoding layer, we exploit spatial information at all corresponding positions to model channel correlations.

3.4. Attention Module Embedding with Networks

In order to take full advantage of long-range contextual information, we aggregate the features from these two attention modules. Specifically, we transform the outputs of two attention modules by a convolution layer and perform an element-wise sum to accomplish feature fusion. At last a convolution layer is followed to generate the final prediction map. We do not adopt cascading operation because it needs more GPU memory. Noted that our attention modules are simple and can be directly inserted in the existing FCN pipeline. They do not increase too many parameters yet strengthen feature representations effectively.

4. Experiments

To evaluate the proposed method, we carry out comprehensive experiments on Cityscapes dataset [5], PASCAL VOC2012 [7], PASCAL Context dataset [14] and COCO Stuff dataset [2]. Experimental results demonstrate that DANet achieves state-of-the-art performance on three datasets. In the next subsections, we first introduce the datasets and implementation details, then we perform a series of ablation experiments on Cityscapes dataset. Finally, we report our results on PASCAL VOC 2012, PASCAL Context and COCO Stuff.

4.1. Datasets and Implementation Details

Cityscapes The dataset has 5,000 images captured from 50 different cities. Each image has 2048×1024 pixels, which have high quality pixel-level labels of 19 semantic classes. There are 2,979 images in training set, 500 images in validation set and 1,525 images in test set. We do not use coarse data in our experiments.

PASCAL VOC 2012 The dataset has 10,582 images for training, 1,449 images for validation and 1,456 images for testing, which involves 20 foreground object classes and one background class.

PASCAL Context The dataset provides detailed semantic labels for whole scenes, which contains 4,998 images for training and 5,105 images for testing. Following [10, 28], we evaluate the method on the most frequent 59 classes along with one background category (60 classes in total).

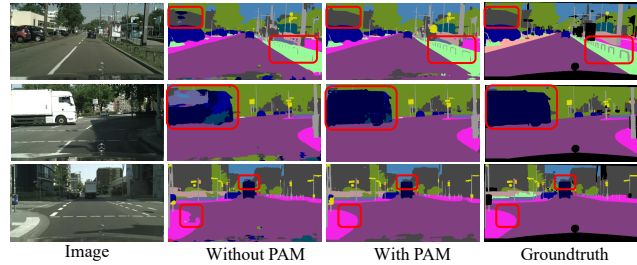


Figure 4: Visualization results of position attention module on Cityscapes val set.

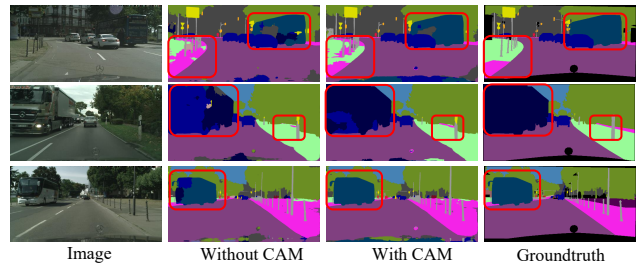


Figure 5: Visualization results of channel attention module on Cityscapes val set.

COCO Stuff The dataset contains 9,000 images for training and 1,000 images for testing. Following [6, 10], we report our results on 171 categories including 80 objects and 91 stuff annotated to each pixel.

4.1.1 Implementation Details

We implement our method based on Pytorch. Following [4, 28], we employ a poly learning rate policy where the initial learning rate is multiplied by $(1 - \frac{iter}{total_iter})^{0.9}$ after each iteration. The base learning rate is set to 0.01 for Cityscapes dataset. Momentum and weight decay coefficients are set to 0.9 and 0.0001 respectively. We train our model with Synchronized BN [28]. Batchsize are set to 8 for Cityscapes and 16 for other datasets. When adopting multi-scale augmentation, we set training time to 180 epochs for COCO Stuff and 240 epochs for other datasets. Following [3], we adopt multi-loss on the end of the network when both two attention modules are used. For data augmentation, we apply random cropping (cropsizes 768) and random left-right flipping during training in the ablation study for Cityscapes datasets.

4.2. Results on Cityscapes Dataset

4.2.1 Ablation Study for Attention Modules

We employ the dual attention modules on top of the dilation network to capture long-range dependencies for better scene understanding. To verify the performance of attention

| Method | BaseNet | PAM | CAM | Mean IoU% |
|-------------|---------|-----|-----|-----------|
| Dilated FCN | Res50 | | | 70.03 |
| DANet | Res50 | ✓ | | 75.74 |
| DANet | Res50 | | ✓ | 74.28 |
| DANet | Res50 | ✓ | ✓ | 76.34 |
| Dilated FCN | Res101 | | | 72.54 |
| DANet | Res101 | ✓ | | 77.03 |
| DANet | Res101 | | ✓ | 76.55 |
| DANet | Res101 | ✓ | ✓ | 77.57 |

Table 1: Ablation study on Cityscapes val set. *PAM* represents Position Attention Module, *CAM* represents Channel Attention Module.

modules, we conduct experiments with different settings in Table 1.

As shown in Table 1, the attention modules improve the performance remarkably. Compared with the baseline FCN (ResNet-50), employing position attention module yields a result of 75.74% in Mean IoU, which brings 5.71% improvement. Meanwhile, employing channel contextual module individually outperforms the baseline by 4.25%. When we integrate the two attention modules together, the performance further improves to 76.34%. Furthermore, when we adopt a deeper pre-trained network (ResNet-101), the network with two attention modules significantly improves the segmentation performance over the baseline model by 5.03%. Results show that attention modules bring great benefit to scene segmentation.

The effects of position attention modules can be visualized in Figure.4. Some details and object boundaries are clearer with the position attention module, such as the 'pole' in the first row and the 'sidewalk' in the second row. Selective fusion over local features enhance the discrimination of details. Meanwhile, Figure.5 demonstrate that, with our channel attention module, some misclassified category are now correctly classified, such as the 'bus' in the first and third row. The selective integration among channel maps helps to capture context information. The semantic consistency have been improved obviously.

4.2.2 Ablation Study for Improvement Strategies

Following [4], we adopt the same strategies to improve performance further. (1) DA: Data augmentation with random scaling. (2) Multi-Grid: we apply employ a hierarchy of grids of different sizes (4,8,16) in the last ResNet block. (3) MS: We average the segmentation probability maps from 8 image scales{0.5 0.75 1 1.25 1.5 1.75 2 2.2} for inference.

Experimental results are shown in Table 2. Data augmentation with random scaling improves the performance by almost 1.26%, which shows that network benefits from enriching scale diversity of training data. We adopt Multi-

| Method | DA | Multi-Grid | MS | Mean IoU% |
|-----------|----|------------|----|-----------|
| DANet-101 | | | | 77.57 |
| DANet-101 | ✓ | | | 78.83 |
| DANet-101 | ✓ | ✓ | | 79.94 |
| DANet-101 | ✓ | ✓ | ✓ | 81.50 |

Table 2: Performance comparison between different strategies on Cityscape val set. *DANet-101* represents DANet with BaseNet ResNet-101, *DA* represents data augmentation with random scaling. *Multi-Grid* represents employing multi-grid method, *MS* represents multi-scale inputs during inference.

Grid to obtain better feature representations of pretrained network, which further achieves 1.11% improvements. Finally, segmentation map fusion further improves the performance to 81.50%, which outperforms well-known method Deeplabv3 [4] (79.30% on Cityscape val set) by 2.20%.

4.2.3 Visualization of Attention Module

For position attention, the overall self-attention map is in size of $(H \times W) \times (H \times W)$, which means that for each specific point in the image, there is an corresponding sub-attention map whose size is $(H \times W)$. In Figure.6, for each input image, we select two points (marked as #1 and #2) and show their corresponding sub-attention map in columns 2 and 3 respectively. We observe that the position attention module could capture clear semantic similarity and long-range relationships. For example, in the first row, the red point #1 are marked on a building and its attention map (in column 2) highlights most the areas where the buildings lies on. Moreover, in the sub-attention map, the boundaries are very clear even though some of them are far away from the point #1. As for the point #2, its attention map focuses on most positions labeled as "car". In the second row, the same holds for the 'traffic sign' and 'person' in global region, even though the number of corresponding pixels is less. The third row is for the 'vegetation' class and 'person' class. In particular, the point #2 does not respond to the nearby 'rider' class, but it does respond to the 'person' faraway.

For channel attention, it is hard to give comprehensible visualization about the attention map directly. Instead, we show some attended channels to see whether they highlight clear semantic areas. In Figure.6, we display the eleventh and fourth attended channels in column 4 and 5. We find that the response of specific semantic is noticeable after channel attention module enhances. For example, 11th channel map responds to the 'car' class in all three examples, and 4th channel map is for the 'vegetation' class, which benefits for the segmentation of two scene categories.

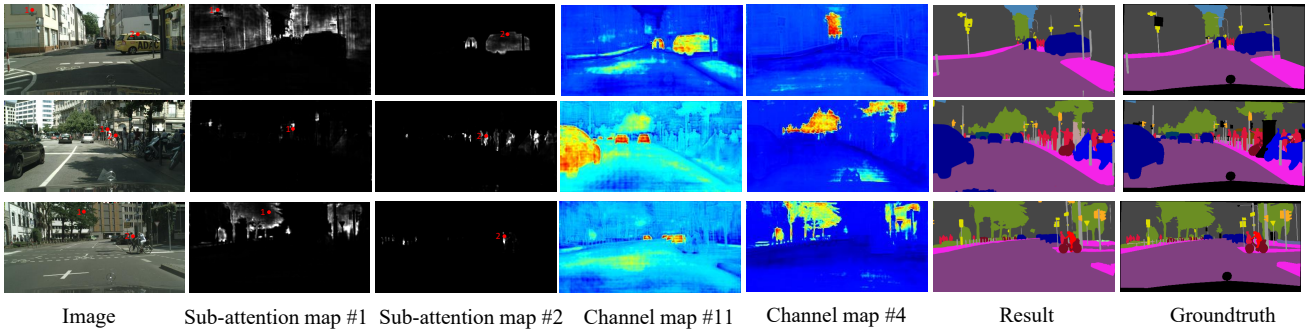


Figure 6: Visualization results of attention modules on Cityscapes val set. For each row, we show an input image, two sub-attention maps ($H \times W$) corresponding to the ponits marked in the input image. Meanwhile, we give two channel maps from the outputs of channel attention module, where the maps are from 4th and 11th channels, respectively. Finally, corresponding result and groundtruth are provided.

| Methods | Mean IoU | | | | | | | | | | | | | | | | | | | |
|----------------|-------------|-------------|-------------|-------------|-------------|-------------|-------------|---------------|--------------|-------------|-------------|-------------|-------------|-------------|-------------|-------------|-------------|-------------|-------------|-------------|
| | | road | sidewalk | building | wall | fence | pole | traffic light | traffic sign | vegetation | terrain | sky | person | rider | car | truck | bus | train | motorcycle | bicycle |
| DeepLab-v2 [3] | 70.4 | 97.9 | 81.3 | 90.3 | 48.8 | 47.4 | 49.6 | 57.9 | 67.3 | 91.9 | 69.4 | 94.2 | 79.8 | 59.8 | 93.7 | 56.5 | 67.5 | 57.5 | 57.7 | 68.8 |
| RefineNet [10] | 73.6 | 98.2 | 83.3 | 91.3 | 47.8 | 50.4 | 56.1 | 66.9 | 71.3 | 92.3 | 70.3 | 94.8 | 80.9 | 63.3 | 94.5 | 64.6 | 76.1 | 64.3 | 62.2 | 70 |
| GCN [15] | 76.9 | - | - | - | - | - | - | - | - | - | - | - | - | - | - | - | - | - | - | - |
| DUC [22] | 77.6 | 98.5 | 85.5 | 92.8 | 58.6 | 55.5 | 65 | 73.5 | 77.9 | 93.3 | 72 | 95.2 | 84.8 | 68.5 | 95.4 | 70.9 | 78.8 | 68.7 | 65.9 | 73.8 |
| ResNet-38 [24] | 78.4 | 98.5 | 85.7 | 93.1 | 55.5 | 59.1 | 67.1 | 74.8 | 78.7 | 93.7 | 72.6 | 95.5 | 86.6 | 69.2 | 95.7 | 64.5 | 78.8 | 74.1 | 69 | 76.7 |
| PSPNet [30] | 78.4 | - | - | - | - | - | - | - | - | - | - | - | - | - | - | - | - | - | - | - |
| BiSeNet [26] | 78.9 | - | - | - | - | - | - | - | - | - | - | - | - | - | - | - | - | - | - | - |
| PSANet [31] | 80.1 | - | - | - | - | - | - | - | - | - | - | - | - | - | - | - | - | - | - | - |
| DenseASPP [25] | 80.6 | 98.7 | 87.1 | 93.4 | 60.7 | 62.7 | 65.6 | 74.6 | 78.5 | 93.6 | 72.5 | 95.4 | 86.2 | 71.9 | 96.0 | 78.0 | 90.3 | 80.7 | 69.7 | 76.8 |
| DANet | 81.5 | 98.6 | 86.1 | 93.5 | 56.1 | 63.3 | 69.7 | 77.3 | 81.3 | 93.9 | 72.9 | 95.7 | 87.3 | 72.9 | 96.2 | 76.8 | 89.4 | 86.5 | 72.2 | 78.2 |

Table 3: Per-class results on Cityscapes testing set. DANet outperforms existing approaches and achieves 81.5% in Mean IoU.

In short, these visualizations further demonstrate the necessity of capturing long-range dependencies for improving feature representation in scene segmentation.

4.2.4 Comparing with State-of-the-art

We further compare our method with existing methods on the Cityscapes testing set. Specifically, we train our DANet-101 with only fine annotated data and submit our test results to the official evaluation server. Results are shown in Table 3. DANet outperforms existing approaches with dominantly advantage. In particular, our model outperforms PSANet [31] by a large margin with the same backbone ResNet-101. Moreover, it also surpasses DenseASPP [25], which use more powerful pretrained models than ours.

4.3. Results on PASCAL VOC 2012 Dataset

We carry out experiments on the PASCAL VOC 2012 dataset to further evaluate the effectiveness of our method. Quantitative results of PASCAL VOC 2012 val set are

| Method | BaseNet | PAM | CAM | Mean IoU% |
|-------------|---------|-----|-----|-----------|
| Dilated FCN | Res50 | | | 75.7 |
| DANet | Res50 | ✓ | ✓ | 79.0 |
| DANet | Res101 | ✓ | ✓ | 80.4 |

Table 4: Ablation study on PASCAL VOC 2012 val set. *PAM* represents Position Attention Module, *CAM* represents Channel Attention Module.

shown in Table. 4. Our attention modules improves performance significantly, where DANet-50 exceeds the baseline by 3.3%. When we adopt a deeper network ResNet-101, the model further achieves a Mean IoU of 80.4%. Following [4, 28, 30], we employ the PASCAL VOC 2012 trainval set further fine-tune our best model. The results of PASCAL VOC2012 on test set is are shown in Table 5.

| Method | Mean IoU% |
|-----------------------------|-------------|
| FCN [13] | 62.2 |
| DeepLab-v2(Res101-COCO) [3] | 71.6 |
| Piecewise [11] | 75.3 |
| ResNet38 [10] | 82.5 |
| PSPNet(Res101) [30] | 82.6 |
| EncNet (Res101) [28] | 82.9 |
| DANet(Res101) | 82.6 |

Table 5: Segmentation results on PASCAL VOC 2012 testing set.

| Method | Mean IoU% |
|------------------------------|-------------|
| FCN-8s [13] | 37.8 |
| Piecewise [11] | 43.3 |
| DeepLab-v2 (Res101-COCO) [3] | 45.7 |
| RefineNet (Res152) [10] | 47.3 |
| PSPNet (Res101) [30] | 47.8 |
| Ding et al.(Res101) [6] | 51.6 |
| EncNet (Res101) [28] | 51.7 |
| Dilated FCN(Res50) | 44.3 |
| DANet (Res50) | 50.1 |
| DANet (Res101) | 52.6 |

Table 6: Segmentation results on PASCAL Context testing set.

4.4. Results on PASCAL Context Dataset

In this subsection, we carry out experiments on the PASCAL Context dataset to further evaluate the effectiveness of our method. We adopt the same training and testing settings on PASCAL VOC 2012 dataset. Quantitative results of PASCAL Context are shown in Table. 6. The baseline (Dilated FCN-50) yields Mean IoU 44.3%. DANet-50 boosts the performance to 50.1%. Furthermore, with a deep pretrained network ResNet101, our model results achieve Mean IoU 52.6%, which outperforms previous methods by a large margin. Among previous works, Deeplab-v2 and RefineNet adopt multi-scale feature fusion by different atrous convolution or different stage of encoder. In addition, they trained their model with extra COCO data or adopt a deeper model (ResNet152) to improve their segmentation results. Different from the previous methods, we introduce attention modules to capture global dependencies explicitly, and the proposed method can achieve better performance.

4.5. Results on COCO Stuff Dataset

We also conduct experiments on the COCO Stuff dataset to verify the generalization of our proposed network. Com-

| Method | Mean IoU% |
|--------------------------|-------------|
| FCN-8s [13] | 22.7 |
| DeepLab-v2(Res101) [3] | 26.9 |
| DAG-RNN [18] | 31.2 |
| RefineNet (Res101) [10] | 33.6 |
| Ding et al.(Res101) [6] | 35.7 |
| Dilated FCN (Res50) | 31.9 |
| DANet (Res50) | 37.2 |
| DANet (Res101) | 39.7 |

Table 7: Segmentation results on COCO Stuff testing set.

parisons with previous state-of-the-art methods are reported in Table. 7. Results show that our model achieves 39.7% in Mean IoU, which outperforms these methods by a large margin. Among the compared methods, DAG-RNN [18] utilizes chain-RNNs for 2D images to model rich spatial dependencies, and Ding et al. [6] adopts a gating mechanism in the decoder stage for improving inconspicuous objects and background stuff segmentation. our method could capture long-range contextual information more effectively and learn better feature representation in scene segmentation.

5. Conclusion

In this paper, we have presented a Dual Attention Network (DANet) for scene segmentation, which adaptively integrates local semantic features using the self-attention mechanism. Specifically, we introduce a position attention module and a channel attention module to capture global dependencies in the spatial and channel dimensions respectively. The ablation experiments show that dual attention modules capture long-range contextual information effectively and give more precise segmentation results. Our attention network achieves outstanding performance consistently on four scene segmentation datasets, i.e. Cityscapes, Pascal VOC 2012, Pascal Context, and COCO Stuff. In addition, it is important to decrease the computational complexity and enhance the robustness of the model, which will be studied in future work.

Acknowledgment

This work was supported by Beijing Natural Science Foundation (4192059) and National Natural Science Foundation of China (61872366, 61472422 and 61872364).

References

- [1] Wonmin Byeon, Thomas M. Breuel, Federico Raue, and Marcus Liwicki. Scene labeling with LSTM recurrent neural networks. In *IEEE Conference on Computer Vision and Pattern Recognition, CVPR*, pages 3547–3555, 2015.

- [2] Holger Caesar, Jasper R. R. Uijlings, and Vittorio Ferrari. Coco-stuff: Thing and stuff classes in context. *CoRR*, abs/1612.03716, 2016.
- [3] Liang-Chieh Chen, George Papandreou, Iasonas Kokkinos, Kevin Murphy, and Alan L. Yuille. Deeplab: Semantic image segmentation with deep convolutional nets, atrous convolution, and fully connected crfs. *IEEE Transactions on Pattern Analysis and Machine Intelligence.*, 40(4):834–848, 2018.
- [4] Liang-Chieh Chen, George Papandreou, Florian Schroff, and Hartwig Adam. Rethinking atrous convolution for semantic image segmentation. *CoRR*, abs/1706.05587, 2017.
- [5] Marius Cordts, Mohamed Omran, Sebastian Ramos, Timo Rehfeld, Markus Enzweiler, Rodrigo Benenson, Uwe Franke, Stefan Roth, and Bernt Schiele. The cityscapes dataset for semantic urban scene understanding. In *IEEE Conference on Computer Vision and Pattern Recognition*, pages 3213–3223, 2016.
- [6] Henghui Ding, Xudong Jiang, Bing Shuai, Ai Qun Liu, and Gang Wang. Context contrasted feature and gated multi-scale aggregation for scene segmentation. In *Proceedings of the IEEE Conference on Computer Vision and Pattern Recognition*, pages 2393–2402, 2018.
- [7] Mark Everingham, Luc Van Gool, Christopher KI Williams, John Winn, and Andrew Zisserman. The pascal visual object classes (voc) challenge. *International journal of computer vision*, 88(2):303–338, 2010.
- [8] Jun Fu, Jing Liu, Yuhang Wang, and Hanqing Lu. Stacked deconvolutional network for semantic segmentation. *arXiv preprint arXiv:1708.04943*, 2017.
- [9] Di Lin, Yuanfeng Ji, Dani Lischinski, Daniel Cohen-Or, and Hui Huang. Multi-scale context intertwining for semantic segmentation. In *Proceedings of the European Conference on Computer Vision (ECCV)*, pages 603–619, 2018.
- [10] Guosheng Lin, Anton Milan, Chunhua Shen, and Ian D. Reid. Refinenet: Multi-path refinement networks for high-resolution semantic segmentation. In *IEEE Conference on Computer Vision and Pattern Recognition*, pages 5168–5177, 2017.
- [11] Guosheng Lin, Chunhua Shen, Anton van den Hengel, and Ian D. Reid. Efficient piecewise training of deep structured models for semantic segmentation. In *IEEE Conference on Computer Vision and Pattern Recognition*, pages 3194–3203, 2016.
- [12] Zhouhan Lin, Minwei Feng, Cicero Nogueira dos Santos, Mo Yu, Bing Xiang, Bowen Zhou, and Yoshua Bengio. A structured self-attentive sentence embedding. *arXiv preprint arXiv:1703.03130*, 2017.
- [13] Jonathan Long, Evan Shelhamer, and Trevor Darrell. Fully convolutional networks for semantic segmentation. In *Proceedings of the IEEE conference on computer vision and pattern recognition*, pages 3431–3440, 2015.
- [14] Roozbeh Mottaghi, Xianjie Chen, Xiaobai Liu, Nam-Gyu Cho, Seong-Whan Lee, Sanja Fidler, Raquel Urtasun, and Alan L. Yuille. The role of context for object detection and semantic segmentation in the wild. In *2014 IEEE Conference on Computer Vision and Pattern Recognition*, pages 891–898, 2014.
- [15] Chao Peng, Xiangyu Zhang, Gang Yu, Guiming Luo, and Jian Sun. Large kernel matters - improve semantic segmentation by global convolutional network. In *IEEE Conference on Computer Vision and Pattern Recognition*, pages 1743–1751, 2017.
- [16] Olaf Ronneberger, Philipp Fischer, and Thomas Brox. U-net: Convolutional networks for biomedical image segmentation. In *Medical Image Computing and Computer-Assisted Intervention*, pages 234–241, 2015.
- [17] Tao Shen, Tianyi Zhou, Guodong Long, Jing Jiang, Shirui Pan, and Chengqi Zhang. Disan: Directional self-attention network for rnn/cnn-free language understanding. In *Proceedings of the Thirty-Second AAAI Conference on Artificial Intelligence*, 2018.
- [18] Bing Shuai, Zhen Zuo, Bing Wang, and Gang Wang. Scene segmentation with dag-recurrent neural networks. *IEEE Trans. Pattern Anal. Mach. Intell.*, pages 1480–1493, 2018.
- [19] Jinhui Tang, Richang Hong, Shuicheng Yan, Tat-Seng Chua, Guo-Jun Qi, and Ramesh Jain. Image annotation by k nn-sparse graph-based label propagation over noisily tagged web images. *ACM Transactions on Intelligent Systems and Technology (TIST)*, 2(2):14, 2011.
- [20] Jinhui Tang, Lu Jin, Zechao Li, and Shenghua Gao. Rgb-d object recognition via incorporating latent data structure and prior knowledge. *IEEE Transactions on Multimedia*, 17(11):1899–1908, 2015.
- [21] Ashish Vaswani, Noam Shazeer, Niki Parmar, Jakob Uszkoreit, Llion Jones, Aidan N. Gomez, Lukasz Kaiser, and Illia Polosukhin. Attention is all you need. In *Advances in Neural Information Processing Systems 30*, pages 6000–6010, 2017.
- [22] Panqu Wang, Pengfei Chen, Ye Yuan, Ding Liu, Zehua Huang, Xiaodi Hou, and Garrison W. Cottrell. Understanding convolution for semantic segmentation. In *IEEE Winter Conference on Applications of Computer Vision*, pages 1451–1460, 2018.
- [23] Xiaolong Wang, Ross Girshick, Abhinav Gupta, and Kaiming He. Non-Local Neural Networks. In *CVPR*, 2018.
- [24] Zifeng Wu, Chunhua Shen, and Anton van den Hengel. Wider or deeper: Revisiting the resnet model for visual recognition. *arXiv preprint arXiv:1611.10080*, 2016.
- [25] Maoke Yang, Kun Yu, Chi Zhang, Zhiwei Li, and Kuiyuan Yang. Denseaspp for semantic segmentation in street scenes. In *Proceedings of the IEEE Conference on Computer Vision and Pattern Recognition*, pages 3684–3692, 2018.
- [26] Changqian Yu, Jingbo Wang, Chao Peng, Changxin Gao, Gang Yu, and Nong Sang. Bisenet: Bilateral segmentation network for real-time semantic segmentation. In *Proceedings of the European Conference on Computer Vision (ECCV)*, pages 325–341, 2018.
- [27] Yuhui Yuan and Jingdong Wang. Ocnet: Object context network for scene parsing. *arXiv preprint arXiv:1809.00916*, 2018.
- [28] Hang Zhang, Kristin Dana, Jianping Shi, Zhongyue Zhang, Xiaoqiang Wang, Amrith Tyagi, and Amit Agrawal. Context encoding for semantic segmentation. In *The IEEE Conference on Computer Vision and Pattern Recognition (CVPR)*, 2018.

- [29] Han Zhang, Ian J. Goodfellow, Dimitris N. Metaxas, and Augustus Odena. Self-attention generative adversarial networks. *CoRR*, abs/1805.08318, 2018.
- [30] Hengshuang Zhao, Jianping Shi, Xiaojuan Qi, Xiaogang Wang, and Jiaya Jia. Pyramid scene parsing network. In *IEEE Conference on Computer Vision and Pattern Recognition*, pages 6230–6239, 2017.
- [31] Hengshuang Zhao, Yi Zhang, Shu Liu, Jianping Shi, Chen Change Loy, Dahua Lin, and Jiaya Jia. Pscanet: Point-wise spatial attention network for scene parsing. In *Proceedings of the European Conference on Computer Vision (ECCV)*, pages 267–283, 2018.